Dicer function is essential for lung epithelium morphogenesis

Kelley S. Harris*, Zhen Zhang*, Michael T. McManus†, Brian D. Harfe‡, and Xin Sun*§

*Laboratory of Genetics, University of Wisconsin, 425-G Henry Mall, Madison, WI 53706; †Department of Microbiology and Immunology Diabetes Center, University of California, 513 Parnassus Avenue, San Francisco, CA 94143; and ‡Department of Molecular Genetics and Microbiology, University of Florida College of Medicine, 1600 SW Archer Road, Gainesville, FL 32610

Communicated by Judith Kimble, University of Wisconsin, Madison, WI, December 15, 2005 (received for review November 11, 2005)

DICER is a key enzyme that processes microRNA and small interfering RNA precursors into their short mature forms, enabling them to regulate gene expression. Only a single *Dicer* gene exists in the mouse genome, and it is broadly expressed in developing tissues. *Dicer*-null mutants die before gastrulation. Therefore, to study *Dicer* function in the later event of lung formation, we inactivated it in the mouse lung epithelium using a *Dicer* conditional allele and the *Sonic Hedgehog*^{cre} (*Shh*^{cre}) allele. Branching arrests in these mutant lungs, although epithelial growth continues in distal domains that are expanded compared with normal samples. These defects result in a few large epithelial pouches in the mutant lung instead of numerous fine branches present in a normal lung. Significantly, the initial phenotypes are apparent before an increase in epithelial cell death is observed, leading us to propose that *Dicer* plays a specific role in regulating lung epithelial morphogenesis independent of its requirement in cell survival. In addition, we found that the expression of *Fgf10*, a key gene involved in lung development, is up-regulated and expanded in the mesenchyme of *Dicer* mutant lungs. Previous studies support the hypothesis that precise localization of FGF10 in discrete sites of the lung mesenchyme serves as a chemoattractant for the outgrowth of epithelial branches. The aberrant *Fgf10* expression may contribute to the *Dicer* morphological defects. However, the mechanism by which DICER functions in the epithelium to influence *Fgf10* expression in the mesenchyme remains unknown.

Fgf10 | microRNA | small interfering RNA

DICER, an RNase III endonuclease, is the enzyme that cleaves microRNA (miRNA) and small interfering RNA (siRNA) precursors into ≈22-nucleotide species (1). This cleavage is an essential step in the biogenesis of these small noncoding RNA molecules. In their mature forms, siRNAs and miRNAs function to regulate gene expression through different mechanisms. siRNAs function by establishing perfect or near-perfect base pairing with their mRNA targets and guiding cleavage of these targets into small RNA fragments. Through this mechanism, endogenous siRNAs silence the expression of the same locus from which they originate ("autosilencing") (1). Although miRNAs can also guide cleavage of target mRNAs, in mammals most miRNAs regulate gene expression by forming imperfect base pairing to sequences in the 3′ UTRs of their target mRNAs, triggering translational repression. Recently, evidence from mammalian cell culture as well as *Caenorhabditis elegans* experiments suggests that miRNAs through translation repression can also cause a decrease in transcripts, likely by facilitating the relocation of the target mRNAs to cytoplasmic compartments, called "P-bodies," where they are degraded (2–4). Regardless of the mechanism, miRNAs silence the expression of target genes at different genomic loci from which they originate ("heterosilencing"). Currently, there are ≈250 miRNAs identified in the mouse genome. They are estimated to regulate the expression of ≈30% of the genes in the genome (5).

Only one *Dicer* gene exists in the mouse genome, which presumably mediates the processing of all miRNAs and endogenous siRNAs. Several mutant alleles of *Dicer* have been generated in mouse, and analyses of their phenotypes demonstrate that *Dicer* functions in multiple developing tissues. *Dicer*-null embryos arrest at embryonic day 7.5 (E7.5) with reduced expression of *Oct4*, an embryonic stem cell marker (6). This finding suggests that *Dicer* is essential for stem cell maintenance in the early embryo. Characterization of a hypomorphic allele of *Dicer* shows that it is essential for angiogenesis (7). Conditional inactivation of *Dicer* in the mouse limb bud mesenchyme led to the conclusion that *Dicer* is essential for cell survival and subsequent formation of proper limb skeletal elements (8). The requirement for *Dicer* in cell survival is consistent with data from cell culture experiments (9).

In this study, we investigate *Dicer* function in lung development. The mammalian lung develops from a ventral evagination of the foregut epithelium into the surrounding splanchnic mesenchyme (10). The nascent lung consists of a proximal trachea and two distal primary buds. As development proceeds, the buds extend and the epithelium undergoes elaborate branching morphogenesis into the adjacent mesenchyme to form the mature lung, which consists of one left lobe and four right lobes. Based on existing evidence, it is proposed that reciprocal signaling between the epithelium and the mesenchyme is crucial for the stereotypical pattern of lung branching (11). A key molecule in this process is FGF10, which is located in the mesenchyme at discrete sites toward which future epithelial branches will grow. *In vitro* data show that FGF10-soaked beads stimulate the outgrowth and chemotaxis of isolated lung epithelium toward the protein source, suggesting that FGF10 functions as a chemoattractant for epithelial branches (12). In addition, FGF10 induces the expression of genes such as *Bmp4* and *Spry2* in the epithelium (12, 13). These molecules, in turn, function to inhibit FGF10 activity, thereby limiting the extent of each outgrowth event.

By RNA *in situ* hybridization, it was shown that *Dicer* is expressed in the developing mouse lung when branching morphogenesis initiates (14). Here we explore *Dicer* function in lung formation by inactivating it in the mouse lung using the Cre/*loxP* approach. Lungs that lack *Dicer* in the epithelium fail to branch normally, demonstrating that *Dicer* is essential for proper lung epithelial morphogenesis.

Results

Inactivation of *Dicer* Function by Using *Shh*^{cre}. To bypass the early embryonic lethality of the *Dicer*-null mutant, we inactivated the gene using an existing conditional allele (8). In this allele (*Dicer*^{flox}), an exon encoding a portion of the second RNaseIII domain is flanked by *lox*P sites (flox). This exon can be deleted upon Cre-mediated recombination. In generating this allele (8),

Conflict of interest statement: No conflicts declared.

Abbreviations: β-gal, β-galactosidase; E*n*, embryonic day *n*; miRNA, microRNA; siRNA, small interfering RNA.

§To whom correspondence should be addressed. E-mail: xsun@wisc.edu.

www.pnas.org/cgi/doi/10.1073/pnas.0510839103

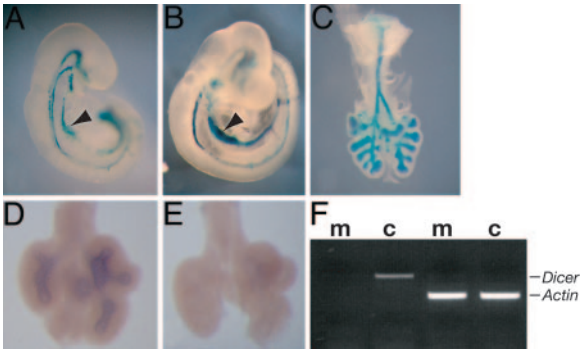

Fig. 1. Cre activity and *Dicer* inactivation. (*A–C*) Cre activity of the Shh^{cre} allele at E9.0 (*A*) and E9.5 (*B*) and in an E12.5 lung (*C*) as assayed by β-gal staining of $Shh^{cre/+}$;*R26R*/+ embryos. Arrowheads indicate prospective lung region. (*D* and *E*) *Dicer* RNA expression in E11.75 control (*D*) and mutant (*E*) lungs as assayed by RNA *in situ* hybridization using a probe hybridizing to the exon that is floxed in the *Dicer* conditional allele. (*F*) RT-PCR of E11.5 control (c) and *Shhcre;Dicer* mutant (m) lung epithelium to illustrate that *Dicer* is inactivated in the mutant at this stage.

it was shown that recombination of this allele in all cells of the embryo phenocopies the reported null allele (6), suggesting that removal of the second RNaseIII domain disrupts DICER function. Furthermore, it was shown that miRNAs are not processed in primary fibroblasts or limb bud mesenchyme homozygous for this recombined allele (8).

To inactivate *Dicer* in the lung epithelium, we used mice carrying the Shh^{cre} allele (15). This allele was generated by insertion of Cre into the *Shh* ORF. Thus, Cre is active in *Shh*-expressing tissues, including the lung. To analyze in detail Shh^{cre} activity in the lung, we mated mice carrying this allele to the R26R reporter mice (16). In $Shh^{cre/+}$;*R26R* embryos, *lacZ* was transcribed in cells that express Cre and in all of the descendants of these cells. At the 14-somite stage (≈E9.0), which is before lung initiation, substantial β-galactosidase (β-gal) activity was detected in the foregut endoderm at the prospective lung region (Fig. 1*A*). At E9.5, when lung outgrowth initiates, β-gal activity was robust in the lung region (Fig. 1*B*). Consistent with this early robust activity, β-gal activity was detected in the entire lung epithelium at E12.5, ≈1 day after lung branching morphogenesis was initiated. No β-gal activity was detected in lung mesenchyme (Fig. 1*C*). These results suggest that the Shh^{cre} allele can be used for efficient Cre-mediated recombination in the lung epithelium before lung initiation.

To address the timing of *Dicer* inactivation by Shh^{cre}, we performed RNA *in situ* analysis using a probe targeted to the deleted exon of *Dicer*. We found that at E10.5 *Dicer* mRNA was detected in both mutant and wild-type lungs (data not shown). At E11.75, however, *Dicer* mRNA was detected in the control lung epithelium ($n = 3/3$) but not in the mutant ($n = 5/5$) (Fig. 1 *D* and *E*). To confirm our *in situ* data, we performed RT-PCR analysis on isolated lung epithelium using primers that are predicted to amplify a PCR product from the wild-type transcript but not the inactivated transcript. At E10.5, a *Dicer* RT-PCR product was detected in both the wild-type and mutant epithelia (data not shown). However, at E11.5, a *Dicer* RT-PCR product was detected only in the wild-type, but not the mutant, epithelium (Fig. 1*F*). These RNA *in situ* and RT-PCR results together indicate that *Dicer* is inactivated between E10.5 and E11.5 in the mutant lung epithelium. This is ≈2.5 days after widespread Cre activity is observed in this region (at E9.0). We speculate that wild-type *Dicer* transcript remains between E9.0 and E11.5 because of either incomplete Cre-mediated recombination or persistence of wild-type *Dicer* transcripts that were synthesized before recombination.

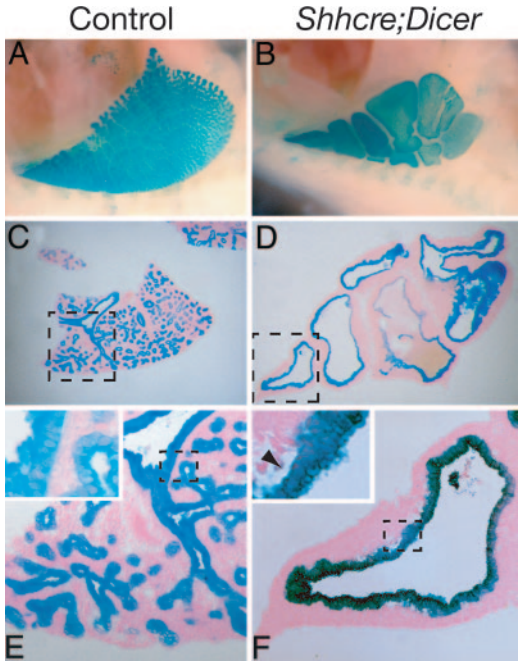

Fig. 2. Morphology of *Shhcre;Dicer* mutant lung. E15.5 lungs shown in whole mount (*A* and *B*, left lobes only) or in plastic sections (*C–F*). Each control and *Shhcre;Dicer* mutant pair is shown at the same magnification. The *R26R* reporter for Cre activity is included in both the control ($Shh^{cre/+}$;$Dicer^{flox/+}$;*R26R*/+) and mutant ($Shh^{cre/+}$;$Dicer^{flox/flox}$;*R26R*/+) lungs. The epithelium is outlined in blue by β-gal staining. Plastic sections are counterstained with eosin to show mesenchymal cells in pink. To ensure penetration of substrate, a control lung lobe was dissected into small pieces before β-gal staining, followed by plastic sectioning. Hence, only a portion of the control lung is captured in the plastic section shown in *C*. *E* and *F* are magnified views of the boxed areas in *C* and *D*, respectively. *Insets* in *E* and *F* are magnified views of the boxed areas within the same panel. The arrowhead in *F* points to a region where the epithelium is detached from the mesenchyme.

***Dicer* Inactivation in Lung Epithelium Results in Dramatic Branching Defects.** To address the defects resulting from *Dicer* inactivation in lung epithelium, we first established $Shh^{cre/+}$;$Dicer^{flox/+}$ lungs as control samples. This is important because the Shh^{cre} allele was generated by insertion of Cre into the *Shh* coding region (15). Thus, only one wild-type copy of *Shh* remains in $Shh^{cre/+}$;$Dicer^{flox/flox}$ (*Shhcre;Dicer*) mutants. We found that *Shhcre;Dicer* mutant mice die at birth and exhibit gross morphological lung defects. In contrast, the $Shh^{cre/+}$;$Dicer^{flox/+}$ control mice are viable and have normal lungs, suggesting that the phenotype observed in the mutant is not a result of loss of one wild-type *Shh* allele and one wild-type *Dicer* allele.

At E15.5, instead of the characteristic tree-like arborization visible in the control lung, the epithelial cells in the mutant lung formed large, fluid-filled sacs within each lobe (Fig. 2 *A* and *B*). Despite this striking branching defect, the mutant lung exhibited a normal lobation pattern. Each lobe maintained a normal shape, albeit proportionally smaller than control samples (Fig. 2 *A* and *B*). Histological sections showed that cells in the epithelium of the E15.5 mutant lung displayed a range of morphologies found in the control lung epithelium, including stratified, pseudostratified, and simple columnar (Fig. 2 *C–F*). Unlike the control lungs, where the epithelium adhered tightly to the mesenchyme, the mutant epithelium was often detached from the mesenchyme.

To define the primary morphogenesis defect in *Shhcre;Dicer* lungs, we examined the epithelial branching phenotype at earlier stages. The outlines of the epithelial cells were visualized with E-cadherin antibody (Fig. 3). We found that the earliest differ-

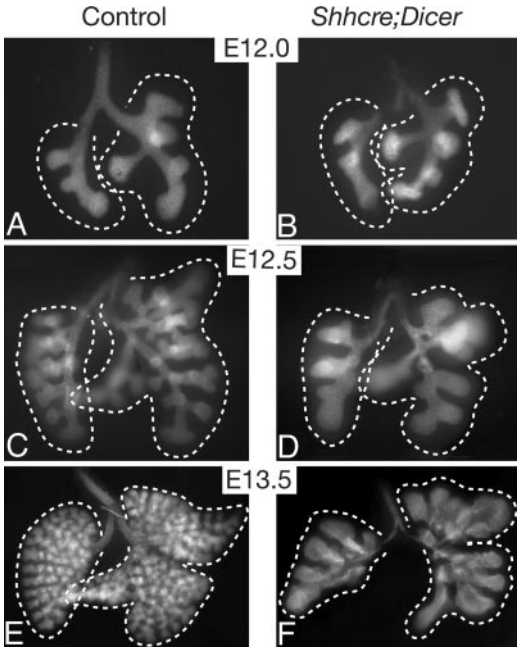

Fig. 3. Epithelial branching patterns in *Shhcre;Dicer* lungs. Epithelial cells are labeled with anti-E-cadherin antibody. At each stage, control and *Shhcre;Dicer* mutant lungs are shown at the same magnification. Branching in the mutant was similar to normal control at E12.0 (*A* and *B*) but was reduced at E12.5 (*C* and *D*) and E13.5 (*E* and *F*). The dashed white lines outline the lung lobes. Note that the overall size of the mutant lung lobes was similar to that of controls at all three stages, even though the epithelial surface area was reduced in the mutant at E12.5 and E13.5 because of reduced branching.

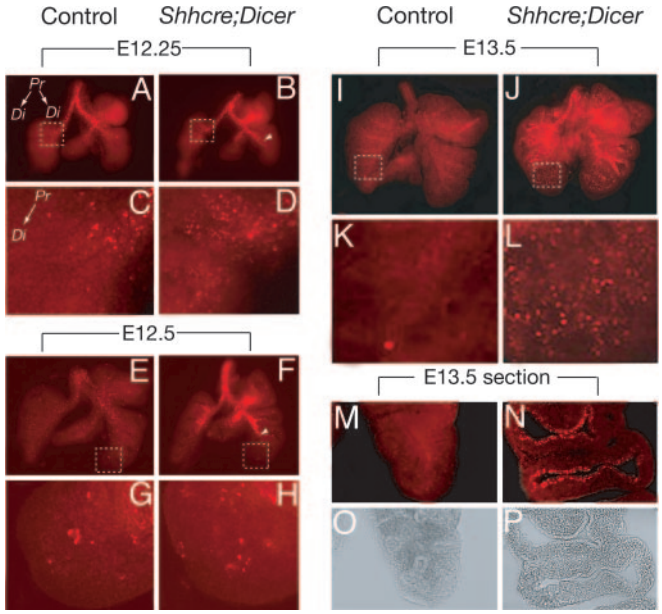

Fig. 4. Cell death analysis of *Shhcre;Dicer* lungs. Cell death was detected by LysoTracker Red staining in whole mount (*A–L*) or vibratome section (*M–P*) at the stages indicated. Each control and mutant pair is shown at the same magnification. *C*, *D*, *G*, *H*, *K*, and *L* are magnified views of the boxed areas in *A*, *B*, *E*, *F*, *I*, and *J*, respectively. *O* and *P* are bright-field images of sections shown in *M* and *N*, respectively. Arrowheads in *B* and *F* indicate the distal extent of the cell death that is present in secondary bronchi. Representative proximal (*Pr*) and distal (*Di*) axes of the lung are indicated in *A* and *C*. In control lungs, cell death was detected in the trachea and primary bronchi at E12.25 but not at E12.5 or later stages. In mutant lungs, cell death was detected in the trachea and primary and secondary bronchi at E12.25 and E12.5. In E13.5 mutant lungs, cell death was detected in the entire lung epithelium but not in the mesenchyme.

ence in branching pattern was observed at E12.5, ≈1 day after *Dicer* inactivation on the mRNA level. In mutant lungs at E12.5 ($n = 6/6$), fewer branches were observed, and the distal tips of the newly formed branches were dilated compared with those of control littermates ($n = 20$) (Fig. 3 *C* and *D*). This phenotype was further exaggerated at E13.5 in the mutant ($n = 2/2$) compared with control ($n = 8$) (Fig. 3 *E* and *F*). The number of dilated branching tips in the E12.5 mutant corresponds to the number of visible sacs at E15.5, suggesting that formation of new branches arrested in the mutant at E12.5, while epithelial growth continued. The size of each of the mutant lung lobes remained normal until E13.5 (Fig. 3 *E* and *F*) and was reduced compared with control after this stage (Fig. 2 *A* and *B* and data not shown).

Prolonged and Ectopic Cell Death Is Observed in the *Dicer* Mutant Lung. *Dicer* is important for maintaining cell survival in culture and in developing limb buds (8, 9). To address whether *Dicer* is important for cell survival in the developing lung, we examined cell death in *Shhcre;Dicer* and control lungs. Using LysoTracker staining to label apoptotic cells, we detected dynamic patterns of cell death in both the control and mutant lungs (Fig. 4).

In control ($Shh^{cre/+};Dicer^{flox/+}$) lungs at E12.25, cell death was detected in the majority of the samples in the trachea and primary bronchi ($n = 11/13$) (Fig. 4 *A* and *C* and data not shown). To address whether this cell death pattern was due to loss of a single allele of *Shh* and/or *Dicer* in the control samples, we examined wild-type (FVB/N background) lungs. In these lungs we detected a similar pattern of cell death at E12.25 ($n = 8/8$) (data not shown), suggesting that proximal cell death is a naturally occurring process during normal lung development. Interestingly, shortly thereafter at E12.5, cell death was no longer detected in the majority of both the control and wild-type lungs ($n = 14/20$ for control, and $n = 8/8$ for wild type) (Fig. 4 *E* and *G*). The same was true at later stages (Fig. 4 *I* and *K* and data not shown), suggesting that normal epithelial cell death occurs only in a restricted time window.

In mutant lungs at E12.25, cell death occurred in the trachea and primary bronchi similar to control and wild type. In addition to this normal pattern, in the mutant cell death extended into the secondary bronchi but not into the distal branching region of the lung ($n = 2/2$) (Fig. 4 *B* and *D*). At E12.5 ($n = 6/6$) (Fig. 4 *F* and *H*) and E12.75 ($n = 4/4$) (data not shown), intense cell death remained in the trachea and bronchi in mutant lungs, even though it was attenuated in the control and wild type. Again, in the mutant lungs, no cell death was observed in the distal branching region. However, by E13.0 ($n = 4/4$) (data not shown) and E13.5 ($n = 2/2$) (Fig. 4 *J* and *L*), aberrant cell death was detected in the entire mutant lung, including the distal branching region. Analysis using vibratome sections showed that this cell death was restricted to the epithelium, where *Dicer* is inactivated (Fig. 4 *M–P*). By E15.5, cell death in the mutant lung was reduced in intensity both proximally and distally (data not shown). The key finding from our cell death analysis is that, in the distal region of the mutant lung, aberrant cell death was first detected at E13.0, after the morphogenesis phenotype became apparent in the same region (E12.5).

***Dicer* Inactivation Leads to Changes in the Expression of Key Signaling Molecules in the Lung.** Our histological and cellular analyses show that *Dicer* is required in the lung epithelium for branching morphogenesis. This conclusion, together with the known role of DICER in processing double-stranded RNAs, led us to hypothesize that the branching phenotype may be explained by misregulation of important branching factors due to the absence of

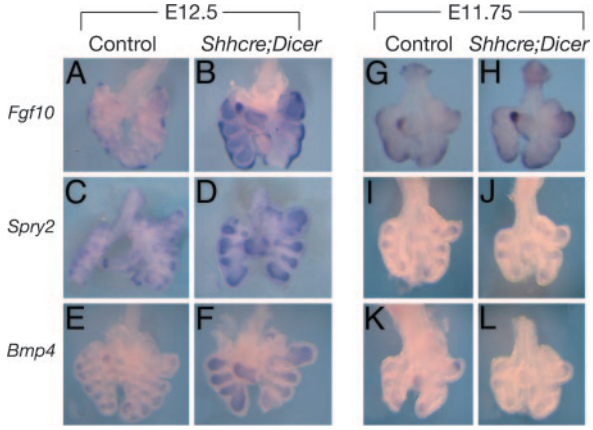

Fig. 5. Gene expression in *Shhcre;Dicer* lungs. Shown is whole-mount RNA *in situ* analysis of *Fgf10*, *Spry2*, and *Bmp4* expression in control and mutant lungs at E12.5 (*A–F*) and E11.75 (*G–L*). At E12.5, the expression of all three genes was increased in the mutant compared with control. At E11.75, *Fgf10* expression was increased in the mutant, whereas *Spry2* and *Bmp4* expression was not changed compared with control. Note that in *B* and *H*, despite *Fgf10* up-regulation, there were still regional differences in expression level within each of the mutant lungs, similar to controls in *A* and *G*.

mature miRNAs or siRNAs. To test this hypothesis, we assayed for the expression of genes known to play a role in branching at E12.5 (Fig. 5). Because this stage precedes apparent cell death in the distal epithelium, any change in gene expression is not likely due to cell death. In a normal developing lung, *Fgf10* is expressed in restricted sites in the mesenchyme whereas both *Spry2* and *Bmp4* are expressed mainly in the distal epithelium. In the mutant, we found that the expression of *Fgf10* was up-regulated in the mesenchyme ($n = 9/9$), and that of *Spry2* and *Bmp4* was up-regulated in the epithelium ($n = 2/2$ and $n = 3/3$, respectively) (Fig. 5 *A–F*).

Because *Spry2* and *Bmp4* gene expression are responsive to FGF10 signaling, their up-regulation may be secondary to that of *Fgf10* (12, 13). To address this possibility, we assayed the expression of these genes at E11.75 before the appearance of the morphogenesis defect described above. We found that *Fgf10* is up-regulated ($n = 4/5$) whereas *Spry2* and *Bmp4* ($n = 2/2$ and $n = 3/3$, respectively) are expressed in the mutant lungs at a level similar to control (Fig. 5 *G–L*). This finding suggests that the up-regulation of *Spry2* and *Bmp4* observed at E12.5 is likely due to the prior increase in *Fgf10* expression. Given the role of FGF10 as a chemoattractant for outgrowth, this up-regulation of *Fgf10* expression is consistent with the branching morphogenesis phenotype observed in the *Dicer* mutant lung.

Discussion

In this study, we inactivated *Dicer* function in lung epithelium shortly after the initiation of lung branching. *Dicer* mutant lungs exhibit two major cellular defects: a disruption in epithelial morphogenesis and an increase in epithelial cell death. Because abnormal cell death in the distal region of the lung is observed at a stage later than the morphogenesis defect, we propose that *Dicer* function is specifically required for epithelial morphogenesis independent of its role in cell survival. *Dicer* may also function in lung initiation and/or cell differentiation. These roles can be investigated by inactivating *Dicer* in the lung at an earlier or a later time than in this study.

In *Shhcre;Dicer* mutant lungs, the increase in cell death is first observed in the proximal epithelium at E12.25 before it is detected in the distal epithelium at E13.0. This difference in timing is intriguing because our analysis of Cre activity (Fig. 1 *A* and *B*) predicts that *Dicer* is inactivated in different regions of the lung epithelium at the same time. A likely explanation for this cell death phenotype is that proximal and distal epithelial cells may have different cell survival requirements. This possibility is supported by our observation that in wild-type developing lungs cell death is observed in the proximal but not distal epithelium at E12.25, before overt cell differentiation. To our knowledge, this transient, endogenous cell death in the proximal lung epithelium has not been described before in published literature. It may represent a process of "epithelial trimming" possibly to prime this cell layer for differentiation. Cell death is similarly essential for other normal developmental events, such as neural tube closure (17). In the future, it will be important to investigate the significance of normal cell death during proximal lung development and the signals regulating this event.

Increased cell death was also detected in the limb buds of limb-specific *Dicer* mutants and was postulated to be responsible for all morphological phenotypes observed in those limbs (8). In contrast, in *Shhcre;Dicer* lungs the morphogenesis defect is observed before increased cell death distally. We focus on cell death in distal lung because outgrowth and branching occurs in this region. Because the cell lineages that give rise to proximal structures (trachea and bronchi) versus distal structures (bronchioles and alveoli) are distinct before lung formation (18), it is unlikely that the increased cell death in the proximal lung, which is detected at an earlier stage than distal cell death, can impact distal epithelium morphogenesis. Although we cannot exclude the idea that a change in proliferation may influence the *Dicer* phenotype, our current data led us to propose that the morphogenesis defects result from dramatic changes in the molecular program for branching. This finding is supported by the observation that the expression of *Fgf10*, *Spry2*, and *Bmp4* is up-regulated in E12.5 *Shhcre;Dicer* lungs (Fig. 5 *A–F*). It is interesting to note that *Spry2* up-regulation is also observed in *Dicer* mutant limb buds (8). As indicated in the limb study, miRNA binding sites are identified in the *Spry2* 3′ UTR, suggesting that *Spry2* expression may be directly regulated by miRNAs present in the limb bud. However, in the *Shhcre;Dicer* mutant lung at E11.75, we found that the expression of *Spry2* is not changed, whereas that of *Fgf10* is up-regulated (Fig. 5 *G–J*). In light of the evidence that *Spry2* is positively regulated by FGF signaling at the transcriptional level (13), it is plausible that *Spry2* up-regulation observed in *Shhcre;Dicer* lungs at E12.5 is due to an earlier increase of FGF10. *Bmp4* is up-regulated in E12.5 but not in E11.75 mutant lungs (Fig. 5 *E*, *F*, *K*, and *L*), consistent with previous findings that this gene is positively regulated in the lung epithelium by FGF signaling from the mesenchyme (19). Our evidence suggests that up-regulation of *Fgf10* in the *Shhcre;Dicer* mutant lungs leads to changes in the expression of other genes that are essential for lung morphogenesis.

Several lines of evidence support the hypothesis that the increase in *Fgf10* expression in *Shhcre;Dicer* lungs contributes to the morphogenesis phenotype. First, *Fgf10* is up-regulated (at E11.75) before any apparent morphological defect (E12.5) (Figs. 3 *C* and *D* and 5 *G* and *H*). Second, given the model that FGF10 functions as a chemoattractant for lung epithelial outgrowth, we postulate that the expansion of the *Fgf10* expression domain in the *Dicer* mutant mesenchyme would stimulate the outgrowth of an extended portion of the distal epithelium, consistent with the phenotype observed. Third, the aberrant *Fgf10* expression pattern can also explain the arrest in new branch formation. In wild-type lungs, it is proposed that *Fgf10* expression is continually shifted to new sites in the mesenchyme, facilitating dynamic changes in the direction of epithelial outgrowth (20). In *Dicer* mutant lungs, as the *Fgf10* expression domain is expanded into most of the distal mesenchymal region, it can no longer shift to new sites of

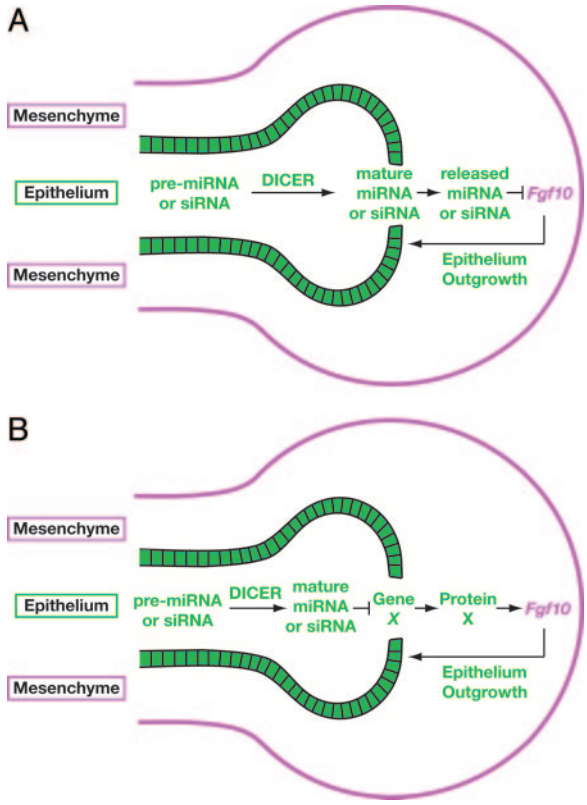

Fig. 6. Two models of DICER function in regulating *Fgf10* expression during lung epithelium morphogenesis. In both models, DICER protein produced in the lung epithelium (green domain) cleaves precursor miRNAs/siRNAs to their mature form. In one model (*A*), we hypothesize that mature miRNA/siRNAs travel to the mesenchyme (purple domain) and directly regulate the expression of target gene *Fgf10*. In an alternative model (*B*), we hypothesize that the mature forms of one or more of the key miRNAs/siRNAs inhibit the expression of a presently unknown gene *X* on the RNA or protein level. We propose that gene *X* encodes a protein that is secreted into the adjacent mesenchyme and functions as a positive regulator of *Fgf10* expression. In both models, FGF10 produced in the mesenchyme then acts as a chemoattractant for epithelium outgrowth and branching. When *Dicer* is inactivated in the lung epithelium, we postulate that the mature form of the key miRNA/siRNA(s) is depleted, leading to an increase of *Fgf10* transcripts. This increase may contribute to the morphogenesis phenotype observed in *Shhcre;Dicer* lungs.

expression. Thus, there is no focal change in the direction of epithelial growth. Although *Fgf10* up-regulation is consistent with the morphological defects observed in the *Shhcre;Dicer* mutant lung, it remains possible that changes in the expression of other genes are responsible for the phenotype.

In considering the possible mechanism of DICER regulation of *Fgf10*, it is important to note that in the *Shhcre;Dicer* lungs *Dicer* is inactivated in the epithelium, whereas *Fgf10* is up-regulated in the mesenchyme. Given the present data, we offer two models for this regulation. In one model (Fig. 6*A*), a key miRNA/siRNA(s) expressed in the epithelium is processed by DICER, then travels to the mesenchyme to inactivate *Fgf10* on the transcriptional and/or translational level. Although systemic transport of small RNAs across cellular boundaries has yet to be demonstrated in mammals, this process is well documented in *C. elegans* (21). According to this model, in the *Dicer* mutant lung, depletion of mature miRNA/siRNAs leads to an increase in the stability of *Fgf10* transcripts. In an alternative model (Fig. 6*B*), a key miRNA/siRNA(s) down-regulates the amount of a secreted protein (protein X) produced in the epithelium. We propose further that, as this target protein is released from the epithelium, it promotes *Fgf10* expression in the mesenchyme. Thus, in the *Dicer* mutant lung, depletion of mature miRNA/siRNAs leads to an increase of the secreted protein, and this in turn up-regulates *Fgf10* expression in lung mesenchyme.

It is significant that our results reveal a mechanism for the regulation of *Fgf10* expression. The current model of lung branching morphogenesis proposes that the precise and dynamic localization of FGF10 defines the stereotypic positions and sequence of lung epithelial branch formation (11, 20). Thus, the regulation of *Fgf10* expression is of key importance in epithelial morphogenesis. However, little is known about the mechanisms that govern this regulation. We note that in *Dicer* mutant lungs, even though there is a general increase in *Fgf10* expression, its level in the distal mesenchyme still varies from region to region (Fig. 5 *B* and *H*), similar to controls. This finding suggests that the underlying positional cue establishing *Fgf10* expression domains in the lung mesenchyme remains in effect, whereas the machinery responsible for attenuating its expression level and restricting its expression domains is disrupted. Future work is needed to elucidate the mechanisms of DICER regulation of *Fgf10* and DICER function in embryonic lung morphogenesis.

Materials and Methods

Generation of *Dicer* Lung Mutants. Mice carrying a conditional floxed allele of *Dicer* (*Dicer^{flox}*) (8) were mated to mice carrying the *Shh^{cre}* allele (15) to generate *Shh$^{cre/+}$;Dicer$^{flox/flox}$* mutant embryos. Offspring were genotyped by using the following PCR primer pairs: for Cre, 5′-TGATGAGGTTCGCAAGAACC-3′ and 5′-CCATGAGTGAACGAACCTGG-3′ (product size: 420 bp); for *Dicer,* 5′-CCTGACAGTGACGGTCCAAAG-3′ and 5′-CATGACTCTTCAACTCAAACT-3′ (product sizes: 420 bp from the *Dicer^{flox}* allele and 351 bp from the wild-type *Dicer* gene).

Embryo Isolation and Phenotype Analyses. Embryos were dissected from time-mated mice, counting noon on the day the vaginal plug was found as E0.5. Whole-mount *in situ* hybridization was performed as described in ref. 22. The *Dicer in situ* probe was prepared from a plasmid containing the entire exon 23 sequence. This exon is removed from the floxed allele upon Cre exposure. For RNA *in situ* analysis of *Fgf10*, *Spry2*, and *Bmp4* expression, E12.5 mutant and control lungs were processed in the same tube using each probe. At E11.75, because mutant and control lungs cannot be distinguished based on morphology, the mutant and control samples were processed in separate tubes, but by using identical aliquoted reagent for each probe. To detect E-cadherin protein, immunofluorescence staining was performed by using a rat anti-E-cadherin antibody (Sigma) as described in ref. 23. To assay Cre activity and label the lung epithelium with β-gal expression, the R26R reporter line (16) was introduced into either the control or the mutant background. β-gal activity was assayed by using a standard protocol. For histological analysis, embryonic lungs were fixed in 4% paraformaldehyde after β-gal staining and embedded in JB-4 plastic resin (Polysciences) according to the manufacturer's protocol. Sections were cut at 5 μm and counterstained with 1% eosin. Areas of cell death were detected by staining with LysoTracker Red DND-99 (Molecular Probes) by using a modified protocol (24). For preparation of vibratome sections, embryonic lungs were fixed in 4% paraformaldehyde for 2 h, embedded in 4% low melting agarose, and sectioned at 50 μm.

RT-PCR Analysis. For normal and *Shhcre;Dicer* mutant embryonic lungs (two pairs each), the epithelium was isolated from the mesenchyme by using a protocol described in ref. 19. Briefly, the embryonic lung buds were dissected in calcium and magnesium-

free PBS (CMF-PBS), incubated in 0.5% trypsin and 1% pancreatin for 5 min at 4°C, then washed in CMF-PBS with 40% FBS. The lung epithelium was then teased from the mesenchyme by using tungsten needles. Total RNA was prepared by using TRIzol (Invitrogen). First-strand synthesis was carried out by using the SuperScript First Strand cDNA Synthesis kit (Invitrogen). PCR was performed by using the following primer pairs: for *β-actin,* 5′-TGGGTCAGAAGGACTCCTATGTG-3′ and 5′-GTGGTACGACCAGAGGCATACAG-3′ (product size: 307 bp); for *Dicer*, 5′-ACCAGCGCTTAGAATTCCTGGGAG-3′ and 5′-GCAGCAGACTTGGCGATCCTGTAG-3′. This *Dicer* primer pair (one hybridizing to the floxed exon 23 and the other to exon 27) is predicted to yield a PCR product (610 bp) from the control transcript, but not the inactivated mutant transcript.

We are grateful to Dr. Cliff Tabin for sharing the *Dicer* conditional allele before publication. We thank Dr. John Fallon and members of the X.S. laboratory for insightful discussions and critical reading of the manuscript. We thank Amber Lashua and Minghui Zhao for excellent technical assistance. We are grateful to Dr. Nobuyuki Itoh (Kyoto University, Kyoto) and Dr. Brigid Hogan (Duke University, Durham, NC) for providing plasmids from which RNA *in situ* probes were prepared. X.S. expresses special thanks to Qun Lu and ChongRong Sun for looking after her F_1 progeny. K.S.H. is supported by David and Lucile Packard Foundation Graduate Scholars Fellowship 2003-24989. This work was supported by Burroughs–Wellcome Career Award 1002361 (to X.S.).

1. Bartel, D. P. (2004) *Cell* **116,** 281–297.
2. Bagga, S., Bracht, J., Hunter, S., Massirer, K., Holtz, J., Eachus, R. & Pasquinelli, A. E. (2005) *Cell* **122,** 553–563.
3. Haase, A. D., Jaskiewicz, L., Zhang, H., Laine, S., Sack, R., Gatignol, A., Filipowicz, W., Pillai, R. S., Bhattacharyya, S. N., Artus, C. G., *et al*. (2005) *EMBO Rep.* **6,** 961–967.
4. Lim, L. P., Lau, N. C., Garrett-Engele, P., Grimson, A., Schelter, J. M., Castle, J., Bartel, D. P., Linsley, P. S. & Johnson, J. M. (2005) *Nature* **433,** 769–773.
5. Lewis, B. P., Burge, C. B. & Bartel, D. P. (2005) *Cell* **120,** 15–20.
6. Bernstein, E., Kim, S. Y., Carmell, M. A., Murchison, E. P., Alcorn, H., Li, M. Z., Mills, A. A., Elledge, S. J., Anderson, K. V. & Hannon, G. J. (2003) *Nat. Genet.* **35,** 215–217.
7. Yang, W. J., Yang, D., Na, S., Sandusky, G., Zhang, Q. & Zhao, G. (2004) *J. Biol. Chem.* **280,** 9330–9335.
8. Harfe, B. D., McManus, M. T., Mansfield, J. H., Hornstein, E. & Tabin, C. J. (2005) *Proc. Natl. Acad. Sci. USA* **102,** 10898–10903.
9. Fukagawa, T., Nogami, M., Yoshikawa, M., Ikeno, M., Okazaki, T., Takami, Y., Nakayama, T. & Oshimura, M. (2004) *Nat. Cell Biol.* **6,** 784–791.
10. Warburton, D., Schwarz, M., Tefft, D., Flores-Delgado, G., Anderson, K. D. & Cardoso, W. V. (2000) *Mech. Dev.* **92,** 55–81.
11. Chuang, P. T. & McMahon, A. P. (2003) *Trends Cell Biol.* **13,** 86–91.
12. Weaver, M., Dunn, N. R. & Hogan, B. L. (2000) *Development (Cambridge, U.K.)* **127,** 2695–2704.
13. Mailleux, A. A., Tefft, D., Ndiaye, D., Itoh, N., Thiery, J. P., Warburton, D. & Bellusci, S. (2001) *Mech. Dev.* **102,** 81–94.
14. Lu, J., Qian, J., Chen, F., Tang, X., Li, C. & Cardoso, W. V. (2005) *Biochem. Biophys. Res. Commun.* **334,** 319–323.
15. Harfe, B. D., Scherz, P. J., Nissim, S., Tian, H., McMahon, A. P. & Tabin, C. J. (2004) *Cell* **118,** 517–528.
16. Soriano, P. (1999) *Nat. Genet.* **21,** 70–71.
17. Weil, M., Jacobson, M. D. & Raff, M. C. (1997) *Curr. Biol.* **7,** 281–284.
18. Perl, A. K., Wert, S. E., Nagy, A., Lobe, C. G. & Whitsett, J. A. (2002) *Proc. Natl. Acad. Sci. USA* **99,** 10482–10487.
19. Weaver, M., Batts, L. & Hogan, B. L. (2003) *Dev. Biol.* **258,** 169–184.
20. Bellusci, S., Grindley, J., Emoto, H., Itoh, N. & Hogan, B. L. (1997) *Development (Cambridge, U.K.)* **124,** 4867–4878.
21. Grishok, A. & Mello, C. C. (2002) *Adv. Genet.* **46,** 339–360.
22. Neubuser, A., Peters, H., Balling, R. & Martin, G. R. (1997) *Cell* **90,** 247–255.
23. Sun, X., Mariani, F. V. & Martin, G. R. (2002) *Nature* **418,** 501–508.
24. Zucker, R. M., Hunter, E. S., III, & Rogers, J. M. (1999) *Methods* **18,** 473–480.